

Generation of the second-harmonic Bessel beams via nonlinear Bragg diffraction

Solomon M. Saltiel^{1,2}, Dragomir N. Neshev¹, Robert Fischer¹, Wieslaw Krolikowski¹, Ady Arie³, and Yuri S. Kivshar¹

¹*Nonlinear Physics Center and Laser Physics Center,
Center for Ultra-high bandwidth Devices for Optical Systems (CUDOS),
Research School of Physical Sciences and Engineering,
Australian National University, Canberra ACT 0200, Australia*

²*Department of Quantum Electronics, Faculty of Physics, Sofia University, Bulgaria and*

³*School of Electrical Engineering, Faculty of Engineering,
Tel-Aviv University, Ramat Aviv, Tel-Aviv, Israel*

We generate conical second-harmonic radiation by transverse excitation of a two-dimensional annular periodically-poled nonlinear photonic structure with a fundamental Gaussian beam. We show that these conical waves are the far-field images of the Bessel beams generated in a crystal by parametric frequency conversion assisted by nonlinear Bragg diffraction.

PACS numbers: 42.65.-k, 42.65.Ky, 42.25.Fx

The second-harmonic generation, i.e. conversion of two photons of the fundamental wave into a single photon at twice the frequency, belongs to one of the most intensively studied nonlinear effects [1]. Such a process takes place in quadratic optical media, i.e. nonlinear media without the center of inversion. It is well established that the efficiency of this as well as other similar parametric processes depends critically on the so-called phase-matching condition which in birefringent crystals is commonly achieved with the temperature or angle tuning. In media with weak birefringence, an efficient frequency conversion is achieved by the quasi-phase matching (QPM) [2]. The QPM technique involves periodic modulation of the second-order nonlinearity of the material. In the ferroelectric crystals such as LiNbO₃ or LiTiO₃, this can be easily realized by spatially periodic poling [3]. In this way one can create one- or two-dimensional nonlinear structures, the so-called $\chi^{(2)}$ photonic crystals [4, 5]. Depending on the symmetry and form of the poling pattern the efficient second-harmonic generation (SHG) can be realized for waves propagating in particular spatial directions [6]. Typical geometries involve, in one spatial dimension, single or multi-period rectangular pattern, and, in two spatial dimensions, nonlinear photonic structures of hexagonal or square symmetries.

In this Letter, we report on the generation of conical second-harmonic waves by excitation of a two-dimensional annular $\chi^{(2)}$ nonlinear photonic fabricated in Stoichiometric Lithium Tantalate (SLT) crystal with a single Gaussian beam. We show that the observed rings of the second-harmonic radiation actually represent the far field of the Bessel beams generated in the crystal via the multi-order nonlinear Bragg diffraction.

We consider a two-dimensional nonlinear photonic structure with circular periodic array of ferroelectric domains with a constant linear refractive index. In general, such two-dimensional QPM photonic structures have been explored exclusively in the *longitudinal* geom-

etry [4, 5, 7, 8] of the second-harmonic generation when the fundamental beam propagates perpendicular to the domains boundaries of periodically varying second-order nonlinearity. Here, we explore a novel *transverse* geometry when the fundamental light beam propagates along the axis of the structure. The front facet of the annular poled Stoichiometric Lithium Tantalate sample used in our experiments with clearly visible domain boundaries is shown in Fig. 1(a) [for technical details, see [7]]. It is a Z-cut, $L = 0.49$ mm thick slab with the QPM period of $7.5 \mu\text{m}$ and duty factor varying inside the sample from 0.7 at Z+ surface to 0.8 at Z-surface. Both, Z+ and Z- surfaces are polished. Small 20 nm deep grooves that remain after polishing cause weak (less than 3%) diffraction of the fundamental beam which we send perpendicular to the domain structure, along its axis. As a light source we use a Ti:Sapphire oscillator and regenerative amplifier delivering beam of 140 fs pulses, with a repetition rate of 250 kHz and average output power of 740 mW. Time bandwidth product of the laser pulses is 0.49.

The input beam is loosely focused such that the beam waist at the input facet of the sample is $147 \mu\text{m}$ (FWHM) which, for a given input power, corresponds to the intensity about 100 GW/cm^2 . The beam covers roughly 10 domain rings. We observe that the transverse illumination of the radial structure by the fundamental beam lead to multiple conical emission of the second-harmonic (SH) waves [see Figs. 1(b) and 2(a)]. These waves form a set of rings in the far field, and their propagation angles satisfy the Bragg relation, i.e they are determined by the ratio of the wavelength of the second harmonic to the period of the modulation of the $\chi^{(2)}$ nonlinearity.

To explain the appearance of the second-harmonic rings, we consider the phase-matching conditions [9] for the corresponding parametric process shown in Fig. 1(c). The general vectorial phase-matching condition can be split into two scalar ones: the transverse condition, $k_2 \sin \alpha_m = G_m = mG_1$, and the longitudinal condition,

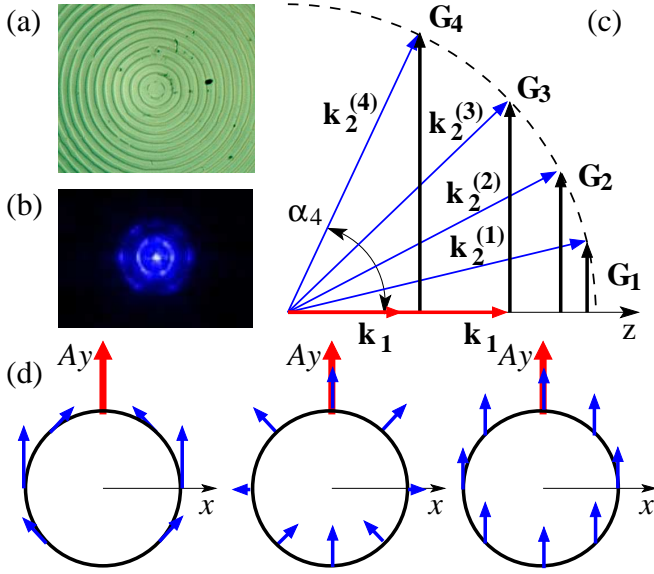


FIG. 1: (color online) (a) Front facet of the SLT sample. (b) Far-field image of first two diffraction SH rings. (c) Phase matching diagram of the SHG process in the transverse QPM grating. (d) Polarization structure of the ordinary (left), extraordinary (middle), and small-angle (right) rings. The fundamental wave (red) has Y polarization.

$k_2 \cos \alpha_m - 2k_1 = \Delta k_m$. With a correct choice of the fundamental wavelength or temperature, a given diffraction order will be longitudinally phase-matched ($\Delta k_m = 0$). As an example, in Fig. 1(c) the third diffraction order is phase-matched ($\Delta k_3 = 0$), and for this interaction both the phase-matching conditions are satisfied simultaneously. Inside the crystal, the propagation angles of all transversely phase-matched waves can be found from the relation $\sin \alpha_m = m\lambda_2/n_2\Lambda$, which is analogous to the Bragg condition governing the diffraction of waves on periodic modulation of the index of refraction. Here the refractive index is constant but the nonlinear properties of the medium experience spatially periodic variations. This effect is known as *nonlinear Bragg diffraction*, and it was first discussed by I. Freund in 1968 [10].

The condition of the total internal reflection determines the maximum number of the second-harmonic rings, $M_1 = \Lambda/\lambda_2$. The SHG process in the transverse direction ($\beta_m = 90^\circ$) determines the total maximum diffraction orders, $M_2 = n_2\Lambda/\lambda_2$. For this transverse SHG process the longitudinal mismatch is $\Delta k_m = 2k_1$, and its compensation is possible only when two counter-propagating fundamental waves are employed [11].

For the annular periodically poled structure, the outer rings possess interesting polarization properties determined by the tensor of the second-order nonlinearity of the Lithium Tantalate. This crystal belongs to the 3m symmetry point group. For the fundamental beam propagating along the Z axis, there exist following nonzero components: $d_{zxx} = d_{zyy}, d_{yxx} = d_{xyx} = -d_{yyy}$. Note

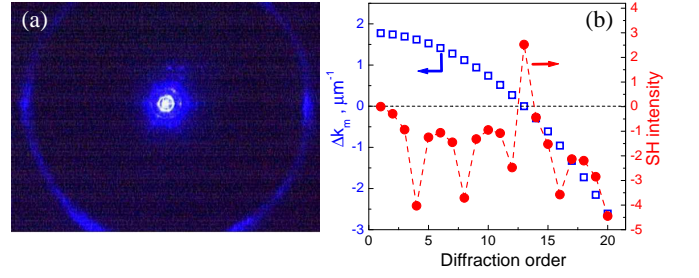


FIG. 2: (color online) Far field image of experimentally observed second-harmonic rings. The axis X is horizontal. (a) Fundamental beam is exactly in the center of the annular structure: first several orders and 13-th order SH ring are seen. (b) Dependencies of the wave vector mismatch and the predicted SH efficiency normalized to the first-order efficiency (in log scale) as a function of the diffraction order.

that in periodically poled crystals with 3m symmetry the values $d_{xxy}, d_{yxx}, d_{yyy}$ also change signs periodically [12]. Two types of the SHG processes are possible: Type I (e-oo, two ordinary waves generate an extraordinary second-harmonic wave) and Type 0 (o-oo, two ordinary waves generate an ordinary second-harmonic wave). Effective nonlinearities for these two processes are [13]

$$d_{\text{eff}}^{(o)} = d_{yyy} \cos(\varphi + 2\gamma), \quad (1)$$

$$d_{\text{eff}}^{(e)} = d_{yyy} \cos \alpha \sin(\varphi + 2\gamma) + d_{zyy} \sin \alpha, \quad (2)$$

where φ is the azimuthal angle measured counterclockwise from the X axis, α is the diffraction angle inside the crystal, and γ is the angle that defines the polarization of the input beam ($\gamma = 0$ for polarization along X axis). The azimuthal intensity distribution of the “ordinary” and “extraordinary” second-harmonic rings is given by $I_{2\omega}^{(o,e)} \propto [d_{\text{eff}}^{(o,e)}]^2 g_m^2 I_1^2 L_{\text{coh}}^2$. Hence, the total intensity is

$$I_{2\omega, m} \propto \left\{ [d_{\text{eff}}^{(o)}]^2 + [d_{\text{eff}}^{(e)}]^2 \right\} g_m^2 I_1^2 L_{\text{coh}, m}^2, \quad (3)$$

where I_1 denotes the intensity of the fundamental beam, $g_m = [2/(\pi m)] \sin(\pi m D)$, $L_{\text{coh}, m} = \pi/\Delta k_m$ and D - represents the duty factor. The light intensity in individual rings depends also on the phase mismatch Δk_m . For ring(s) for which both the phase-matching conditions are fulfilled the coherence length L_{coh} has to be replaced by the actual crystal length L . In Fig. 2(b) we illustrate the dependence of the relative intensity (in log scale) in each diffraction order on m .

For small angles α (when $\tan \alpha \ll 1$), the difference in the refractive indices of the ordinary and extraordinary waves can be neglected, the “ordinary” and “extraordinary” SH rings perfectly overlap, and as a result the intensity of conically emitted light does not depend on γ and φ . In addition, its polarization becomes linear [Fig.

1(d, right)]. For $\gamma = 0$ and for $\gamma = \pi/2$ polarization of the SH wave coincide with the Y -direction (with relevant nonlinear components d_{yx} and d_{yy} , respectively), while for $\gamma = \pi/4$ polarization of the SH wave coincide with the X -direction (with relevant nonlinear component d_{xx}).

For relatively large α , the ordinary and extraordinary waves propagate with different phase velocities [$n_o > n_e(\alpha)$] and at slightly different conical angles. In this case, the output polarization depends strongly on the actual spatial overlap of the two rings since they are orthogonally polarized. In Fig. 1(d) we show the structure of the predicted polarization on the ring for $d_{yy}/d_{zy} \approx -1.7$ [14] and $\alpha = 20^\circ$. For relatively long crystals every diffraction order should appear as a doublet consisting of two orthogonally-polarized rings.

A full analysis of the SHG process in the QPM structure with the azimuthal symmetry shows that, in fact, the SH field inside the crystal has a form of a nondiffracting Bessel beam [15]. Detailed form depends on the crystal symmetry. In the considered earlier case of Strontium Barium Niobate, the SH wave is just the first-order Bessel function with a perfect radial polarization [9]. On the other hand, in case of LiTaO₃ or LiNbO₃, the beam structure is more complicated due to the contributions of several components of the $\chi^{(2)}$ tensor. However, it still can be represented in terms of a superposition of the low-order Bessel functions with the angularly modulated intensity. The exact formulas are quite cumbersome, but they can be simplified in case of small emission angles ($\tan \alpha \ll 1$),

$$E(\rho, \theta_0, z) \propto 2\pi A^2 d_{yy} J_0(\xi) [\hat{u}_x \sin 2\gamma + \hat{u}_y \cos 2\gamma], \quad (4)$$

where $\xi = k_2 \rho \sin \alpha$ and $\rho = (x^2 + y^2)^{1/2}$ is the transverse radial coordinate. \hat{u}_x and \hat{u}_y are unit vectors along X and Y . It is clear that the beam represented by Eq. (4) is linearly polarized, with its intensity being independent of the azimuthal coordinate $I \propto 4\pi^2 d_{yy}^2 A^4 J_0^2(\xi)$. This results are in a full agreement with experimental observations [Fig. 4(d)].

The observed SH rings for the fundamental wavelength of 822 nm are shown in Fig. 2(a). The measured conical angles agree well with those determined from the nonlinear Bragg diffraction formula. By re-scaling the size of the lower-order diffraction pattern we found that the phase matched SH emission which is represented in the far-zone by the ring with the largest diameter and conical angle of 45.6° corresponds to the high 13-th diffraction order. In Fig. 2(b) we depict the calculated (using the published refractive index data [16]) longitudinal phase mismatch and relative power of the SH waves for $\lambda = 836$ nm. The highest peak corresponds to the phase-matched ($\Delta k_{13} = 0$) 13-th order SH ring.

The phase-matching curve is shown in Fig. 3(a) together with the theoretical prediction based on the model from Ref. [9]. We observe good qualitative agreement

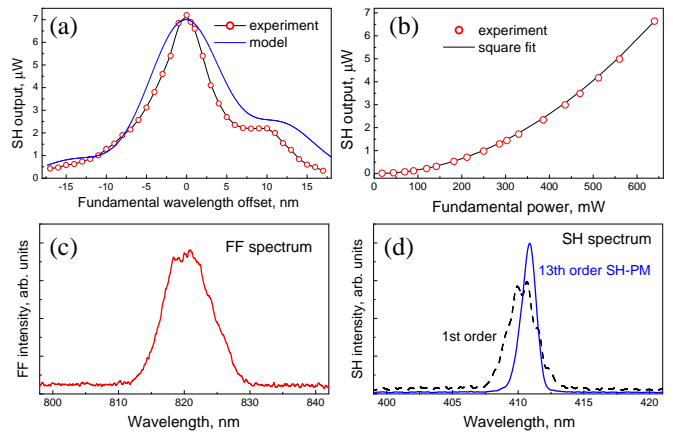


FIG. 3: (color online) (a) Experimentally measured (circles) and theoretically predicted (solid line) phase matching curves. (normalized to the maximum signal of the experiment). (b) Quadratic dependence of the 13-th order SH ring on input power. (c) Spectrum of the fundamental pulse. (d) Spectra of the SH rings for non phase matched (first-order) and phase matched (13-th order) SH ring.

between the experimental curve and the theoretical prediction. In Fig. 3(b) we verify a quadratic dependence of the SH power of the phase matched 13-th SH ring as a function of the input power. From this figure (obtained at 640 mW fundamental average power taking into account all losses), we obtain the internal efficiency for the phase-matched emission of $\eta_{13} = 0.0056\% / \text{W}$. Such low efficiency is attributed to the fact that we use high order QPM interaction. Additionally, the variations of the duty factor inside the crystal leads to an effective length 2-3 times less than the real sample thickness. The measured efficiency of the SH power generated in the first-order ring is 220 times less than η_{13} . The spectra are shown in Fig. 3(c,d). The fundamental spectral width is 8 nm. The spectra of the SH ring in the case of phase-matching of the 13-th order is 1.3 nm; i.e. almost 2 times less than expected for a stationary process. This indicates that the SHG process takes place in the group-velocity mismatch conditions. Indeed, the calculated group-velocity-mismatch length is 0.092 mm for 140 fs fundamental pulse width, that is a half of the expected effective length of the sample. Subsequently, the output spectra (pulse length) is expected to be reduced (stretched) by a factor of 2. In contrast, the spectra of non-phase matched rings [see Fig. 3(d)] do not show any reduction and are close to those predicted for the stationary process, $\Delta\omega_{\text{SH}} = \sqrt{2}\Delta\omega_{\text{FF}}$.

The rings are sensitive to the axial alignment of the fundamental beam. With the off-center beam, the rings transform into a two-peak structure, the efficiency increases, and the number of the observed diffracted orders increases too. For a horizontal shift of the sample, the diffraction spots appear horizontally. For a vertical shift of the sample, the diffraction spots appear vertically.

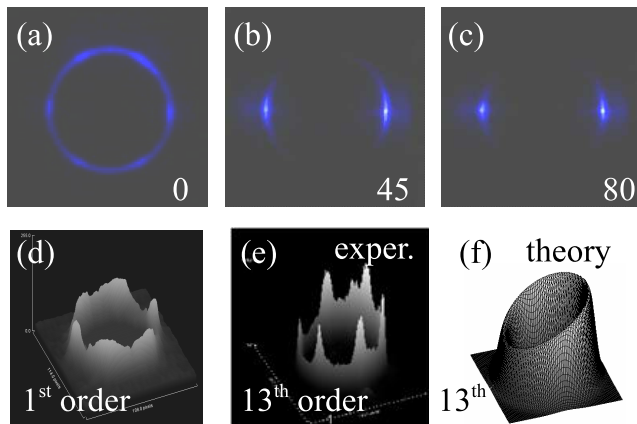


FIG. 4: (color online) (a-c) Modification of the diffraction pattern as a function of the horizontal misalignment of the incident beam. Numbers indicate the shift in μm . The crystallographic X axis is horizontal. (d,e) Experimentally recorded intensity distribution of $m = 1$ and $m = 13$ SH rings. (f) Theoretical prediction for the azimuthal intensity distribution of the $m = 13$ SH ring evaluated from Eq. (3).

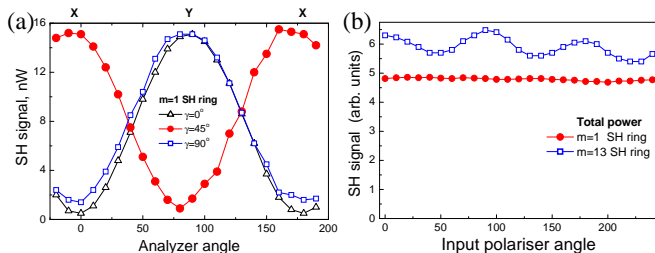


FIG. 5: (color online) Polarization properties of the SH rings: (a) Power of the 1-st order SH ring vs. analyzer angle, (b) Total power of the 1-st and 13-th order SH rings vs. the input polarization angle.

This is explained by the fact that the structure resembles a one-dimensional grating formed from the sectors situated close to the horizontal (vertical) diameter of the rings. The modifications of the diffraction pattern for the phase-matched 13-th order ring in the case of off-center excitation are shown in Figs. 4(a-c). Figures 4(d,e) show the experimental intensity distribution of the 1-st and 13-th order rings. The theoretical prediction for the 13-th order ring is given by Eq. (3), and it is shown in Fig. 4(f).

As follows from Fig. 1(b) and Figs. 4(a,d,e), the second-harmonic rings exhibit an additional azimuthal modulation with 6 well defined peaks. These peaks are insensitive to the input polarization and intensity, and they appear even in the regime of linear diffraction of the fundamental beam on the 20 nm deep surface relief replica of poling pattern. The peaks are artifacts of the discrete character of domain boundaries resulting from the well known tendency of ferroelectric domains in the

SLT to retain their hexagonal shape [7, 17].

In Fig. 5 we show our results of the polarization measurements of the second-harmonic rings. For the linearly polarized input fundamental beam the generated wave is also linearly polarized in the case of the first-order ring. This result agrees with Eqs. (1) and (2) in the limit $\alpha \rightarrow 0$. Polarization state becomes more complex for higher-order nonlinear diffraction as the output signal contains both ordinary and extraordinary contributions.

In conclusion, we have reported on the first observation of the second-harmonic Bessel beams generated by two-dimensional annular nonlinear photonic structures. We have explained the effects observed in experiment by employing the concept of nonlinear Bragg diffraction combined with the longitudinal and transverse phase matching conditions. We have studied the polarization properties of the conical second-harmonic radiation and describe how the beam polarization depends on the crystal symmetry and conical angle.

This work was supported by the Australian Research Council and the Israeli Science Foundation (grant no. 960/05). We thank D. Kasimov, A. Bruner, P. Shaier, and D. Eger for their assistance in the fabrication of the SLT samples. S. Saltiel thanks Nonlinear Physics Center for hospitality and support.

-
- [1] P. A. Franken and J.F. Ward, *Rev. Mod. Phys.* **35**, 23 (1963).
 - [2] M.M. Fejer, G.A. Magel, D.H. Jundt, and R.L. Byer, *IEEE J. Quant. Electron.* **QE-28**, 2631-2654 (1992).
 - [3] M. Houe and P. D. Townsend, *J. Phys. D: Appl. Phys.* **28**, 1747 (1995);
 - [4] V. Berger, *Phys. Rev. Lett.* **81**, 4136-4139 (1998).
 - [5] P. Xu, S. H. Ji, S. N. Zhu, X.Q. Yu, J. Sun, H.T. Wang, J. L. He, Y.Y. Zhu, and N. B. Ming, *Phys. Rev. Lett.* **93**, 133904 (2004).
 - [6] J.R. Kurz, A.M. Schober, D.S. Hum, A.J. Saltzman, and M.M. Fejer, *IEEE Journal of Selected Topics in Quantum Electron.* **8**, 660-664 (2002).
 - [7] D. Kasimov *et al.*, *Opt. Express* **14**, 9371 (2006).
 - [8] N.G.R. Broderick *et al.*, *Phys. Rev. Lett.* **84**, 4345 (2000).
 - [9] S. Saltiel, W. Krolikowski, D. Neshev, Y.S. Kivshar, *Opt. Express* **15**, 4132 (2007).
 - [10] I. Freund, *Phys. Rev. Lett.* **21**, 1404 (1968).
 - [11] R. Fischer *et al.*, *Appl. Phys. Lett.* **91**, 031104 (2007).
 - [12] A. Ganany *et al.*, *Appl. Phys. B* **85**, 97 (2006).
 - [13] F. Zernike and J.E. Midwinter, *Applied Nonlinear Optics* (Wiley, New York, 1973).
 - [14] F. Charra and G.G. Gurzadyan, In: *Nonlinear Dielectric Susceptibilities*, ed. D.F. Nelson (Springer, Berlin, 2000).
 - [15] J. Durnin, *J. Opt. Soc. Am. A* **4**, 651 (1987); Z. Bouchal and M. Olivik, *J. Mod. Optics* **42**, 1555-1556 (1995).
 - [16] M. Nakamura *et al.*, *Jpn. J. Appl. Phys.* **41**, 465 (2002).
 - [17] A.I. Lobov *et al.* <http://eprints.soton.ac.uk/42411/>